Semester project report: Simulations for one ion experiments

Matteo Marinelli

1 Introduction

In the last few decades many experimental and theoretical reports have shown the ability to coherently control the quantum state of trapped ions. It has been shown that ions are a versatile tool to implement quantum logic and quantum computation experiment. Indeed, many important goals have been achieved in this direction such as the realization of Rabi oscillation and Ramsey fringes experiment, universal quantum gates (single qubit rotations, CNOT gate, Toffoli gate, etc...), entanglement among many ions, quantum error correction and quantum teleportation. However, there has been proposal also for "engineering" ionic state of motion like coherent states or other nonclassical states such as squeezed states.

The focus of this report will be on describing the way of implementing such motional states. Before going any further it is worth to spend few words on the quantum mechanical description of trapped ions.
Due to their net charge it is possible to trap ions using a well defined arrangement of electromagnetic fields. In recent experiments, the most used trap is the so called Paul trap, which uses a combination of rf and static fields to confine the ion in all the three directions. When neglecting the micro motion and assuming small jiggling around the equilibrium position, the trap potentials can be considered quadratic and therefore the ion behaves as if it was confined in a static harmonic potential in the radial direction given by[1, 2]:

$$q\Phi_p = \frac{1}{2}m\omega_r^2(x^2 + y^2). \tag{1}$$

Therefore, for practical purpose, the motion is described as the quantum mechanical oscillator. The Hamiltonian describing the motion in the i direction is:

$$\hat{H}_{mot} = \hbar w_i(\hat{a}^\dagger\hat{a} + \frac{1}{2}), \tag{2}$$

where a and $a^\dagger$ are the rising and lowering operator of the quantum harmonic oscillator, and w_i is the trapping frequency in a particular direction. Usually for further usage of

this equation the vacuum contribution will be neglected. A typical trapping frequency is $w_z \simeq 2\pi \cdot 1\text{MHz}$.
The motional states described by this Hamiltonian are crucial for trapped ion physics because they come into play when creating quantum logic operations like entanglement or two qubit gates.

An other important feature that makes the ions so important for quantum information purpose are the internal states. In its simple description an ion can be seen as a two level system, where we consider a ground state level and long lived excited state. For example in the calcium ion it is possible to consider a system created by the Zeeman splitting of the ground state or the quadrupole transition between the $S_{\frac{1}{2}}$ and the $D_{\frac{5}{2}}$ states (transition frequency $w_a \simeq 400\text{THz}$). Or alternately one can use the hyperfine splitting of atoms like Be, where the transition frequency is around 1GHz.
For such a simple system the Hamiltonian reduces to

$$\hat{H}_{int} = \frac{1}{2}\hbar\omega_a\sigma_z, \tag{3}$$

where ω_a is the transition frequency from the ground state and the excited one and σ_z is the Pauli operator for the z-component of the spin.

Connecting together the two description it is possible to describe the ion as a two level system coupled to an harmonic oscillator; therefore it is possible to draw the energy level diagram as the one presented in Fig 1.

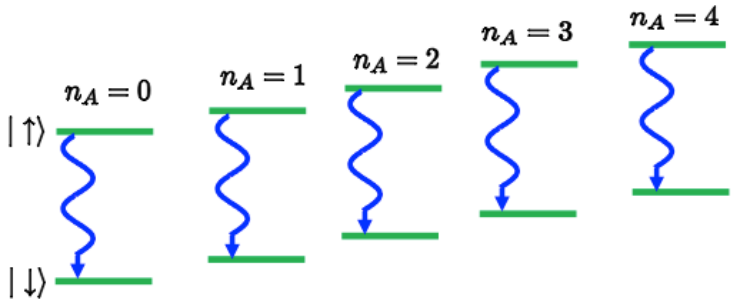

Figure 1: Dressed state diagram.

2 Methods

2.1 Laser hamiltonian

The way to manipulate the quantum system of trapped ions is by using a laser light that couples to the internal and motional states of the atom.

The general interacting Hamiltonian describing the coupling between light and ion is[2]:

$$\hat{H}_I = -i\omega_a A_0 e \ \langle \Phi_i | e^{i\mathbf{k}\cdot\mathbf{R}} | \Phi_j \rangle \mathbf{e_c} \cdot \langle e | \mathbf{r} | g \rangle | \Phi_j \rangle \langle \Phi_i | \hat{a} \ \sigma_+ + h.c. \ , \tag{4}$$

where $|\Phi_i\rangle$ represent the motional state of the ion. Note that differently from the case of interaction with free atoms, the action of the $e^{ik\cdot R}$ on the motion is still unevaluated.

Since that for the ion control is used a laser light instead of a low photon source, it follows that it is like applying a displacement operator ($D(\alpha)$) to the Hamiltonian. In particular the action of $D(\alpha)$ on the annihilation operator $\hat{a}$ is:

$$D(\alpha)\hat{a}D(-\alpha) = \hat{a} + \alpha \ , \tag{5}$$

where α is the coherent amplitude that is typically very large. This allow us to neglect the the term with $\hat{a}$ leaving only the classical term in α. Note that this term evolves like $e^{-i\omega_l t}$. Thanks to this approximation it is possible to rewrite the Hamiltonian as:

$$H_I = \frac{\hbar\Omega_0}{2} e^{i\mathbf{k}\cdot\mathbf{R}} e^{-i\omega_l t}\sigma_+ + h.c. \tag{6}$$

where I introduced the definition of the Rabi frequency Ω_0.

2.2 Lamb Dicke parameter and LD approximation

The only unknown term in Eq.(6) is the $e^{i\mathbf{k}\cdot\mathbf{R}}$ term. By expanding the scalar product as

$$\mathbf{k}\cdot\mathbf{R} = k_x x_0 e^{i\omega_x t} + k_y y_0 e^{i\omega_y t} + k_z z_0 e^{i\omega_z t} \ , \tag{7}$$

one immediately sees that the influence of the laser in any given direction depends on the angle between the wave vector and that particular component. What is typically done is to choose a laser direction such that is only resonant with one component. This allow us to neglect the other terms in the sum.

An other way of writing this scalar product is [2]:

$$\mathbf{k}\cdot\mathbf{R} = \sum_{\alpha=(x,y,z)} \eta_\alpha (\hat{a}_\alpha^\dagger + \hat{a}_\alpha) \ , \tag{8}$$

where η_α is the so called Lamb-Dicke parameter. Remembering that the atom is trapped in an harmonic potential, so $x = \sqrt{\frac{\hbar}{2m\omega_x}}(\hat{a}^\dagger + \hat{a})$ it follows that

$$\eta_x = |\mathbf{k}| cos\theta \sqrt{\frac{\hbar}{2m\omega_x}} \ . \tag{9}$$

Thanks to this definition is possible to write

$$e^{i\mathbf{k}\cdot\mathbf{R}} = e^{i\eta(\hat{a}^\dagger + \hat{a})} \ . \tag{10}$$

Plugging this last result in Eq.(6) and going in the interaction picture with respect to the bare Hamiltonian $H_0 = \hbar\omega_z(\hat{a}^\dagger\hat{a} + \frac{1}{2}) + \frac{1}{2}\hbar\omega_a\sigma_z$ one gets:

$$H_I = \frac{\hbar\Omega_0}{2} e^{i\eta(\hat{a}^\dagger e^{i\omega_z t} + \hat{a}e^{-i\omega_z t})} e^{-i\omega_l t}\sigma_+ e^{i\omega_a t} + h.c. \ , \tag{11}$$

or by expanding the exponential

$$H_I = \frac{\hbar\Omega_0}{2}(1 + i\eta(\hat{a}^\dagger e^{i\omega_z t} + \hat{a}e^{-i\omega_z t}) + \dots) e^{-i\omega_l t}\sigma_+ e^{i\omega_a t} + h.c. \ . \tag{12}$$

Written in this form, and adopting the *rotating wave approximation*, it is possible to identify different types of transition. The *carrier* transition is driven by having $\omega_l = \omega_a$ and the Hamiltonian reads

$$H_I = \frac{\hbar\Omega_0}{2}(1 - \eta^2(\hat{a}^\dagger\hat{a} + \hat{a}\hat{a}^\dagger) + \dots)\sigma_+ + h.c. \ . \tag{13}$$

The second transition is the *red sideband*. In this case $\omega_l = \omega_a - \omega_z$ and the hamiltonian is

$$H_I = \frac{\hbar\Omega_0}{2}(i\eta\hat{a} + \dots)\sigma_+ + h.c. \ . \tag{14}$$

The last one instead is the *blue sideband* and it is characterized by having $\omega_l = \omega_a + \omega_z$ and an Hamiltonian of the form

$$H_I = \frac{\hbar\Omega_0}{2}(i\eta\hat{a}^\dagger + \dots)\sigma_+ + h.c. \ . \tag{15}$$

A fundamental thing to notice is that the Rabi frequency in all the three cases is strongly dependent on the motional level. This means that if the ion is in a thermal state with a large variance one has to account for the different evolution frequency of every motional level.

A typical approximation that is done is the so called *Lamb-Dicke approximation* that consists in neglecting all the terms higher than the second in the expansion of the exponential. Of course this is only valid if η is very small or if the ion is cooled down to the lowest motional levels. As shown later, this is an important thing to bear in mind especially when dealing with large coherent states or with strongly squeezed states.

2.3 Dispersive regime

A powerfull tool used throughout this semester project is the *dispersive regime*, that consists in enhancing the spontaneous emission of the internal state of the ion. This effect is very similar to the Purcell effect[2, 5]. The difference is that in this case the enhancement is achieved by using a laser field that couples the excited state of the ion $|e\rangle$ to a third state $|f\rangle$ that decays with a high rate to the ground state $|g\rangle$. In Fig.2 is given the level scheme of the Ca^+ ion with the coupling lasers [5].

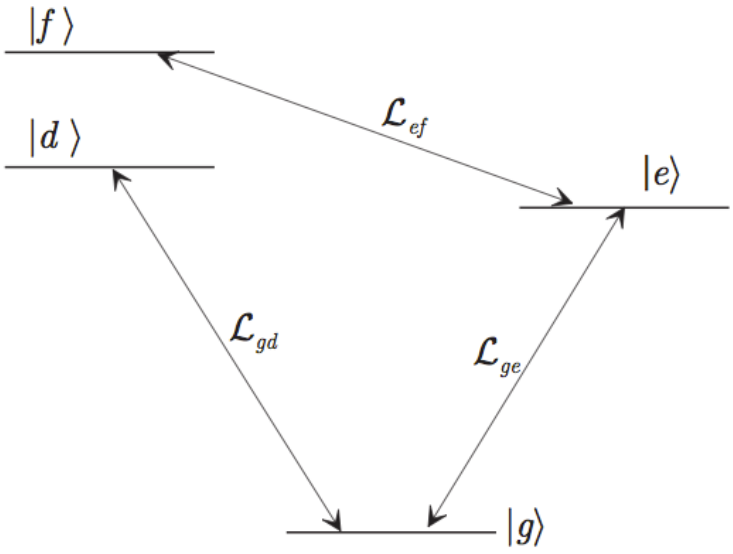

Figure 2: Level scheme for Ca^+ ion. The $|f\rangle \rightarrow |g\rangle$ transition is a dipole allowed transition.[5]

In analogy to the Purcell effect it is possible to define the enhanced spontaneous emission of the excited state $|e\rangle$ as

$$\Gamma_e = \frac{\Omega_{eg}^2}{\Gamma_{fg}} \ , \tag{16}$$

where it is assumed that the spontaneous emission Γ_{eg} is negligible and $\Omega_{eg} \ll \Gamma_{fg}$.

Thanks to this definition is possible to write down the evolution of the density matrix as:

$$\frac{d\rho}{dt} = -\frac{i}{\hbar}\left[H, \rho\right] + \frac{\Gamma_e}{2}(2\sigma_-\rho\sigma_+ - \rho\sigma_+\sigma_- - \sigma_+\sigma_-\rho) \ . \tag{17}$$

Note that in this equation the recoil of the ion is not taken into account. Indeed, for the

purpose of this section, is worth considering only the spontaneous decay term. For a more general evolution see the next chapters.

Solving this equation in a general case is not easy. A typical approximation used to approach the problem is called *adiabatic elimination* and consist neglecting the excited state $|e\rangle$ population. Such approximation is possible because of the strong decay rate.

In the next chapters I will provide a simple derivation of this process when applying a red sideband transition ($\omega_l = \omega_a - \omega_z$). This can be easily extended to the other types of transition that will be used for engineering complex motional states.

3 Sideband cooling

In this chapter I will show how to cool the ion to its motional ground state. Reaching this limit is of crucial importance because it shows how well the ion can be controlled and it is also the starting point for many quantum logic gates. This state can be reached working in the dissipative regime and applying a red sideband transition ($\omega_l = \omega_a - \omega_z$).

As a starting point I will first show a simple derivation for the *adiabatic elimination* of the excited state $|e\rangle$ in the case of interest. Secondly I will show the general hamiltonian used in the simulation and the obtained results[5].

There are two basic assumptions for the derivation: the first is the LD approximation, and the second is that the sideband coupling is smaller than the enhanced spontaneous emission:

$$\frac{\Omega_0 \eta}{2} \ll \Gamma_e \ . \tag{18}$$

Knowing that $\rho = \sum \rho_{ij} |i\rangle\langle j|$, and taking into account Eq.(14) and Eq.(17) it easy to verify the following Bloch equations[5]:

$$\frac{d\rho_{gg}}{dt} = \frac{\Omega_0 \eta}{2}(\hat{a}^\dagger \rho_{eg} + \rho_{ge}\hat{a}) + \Gamma_e \rho_{ee} \ , \tag{19}$$

$$\frac{d\rho_{eg}}{dt} = \frac{\Omega_0 \eta}{2}(\hat{a}\rho_{gg} + \rho_{ee}\hat{a}^\dagger) - \frac{\Gamma_e}{2}\rho_{ee} \ , \tag{20}$$

$$\frac{d\rho_{ee}}{dt} = \frac{\Omega_0 \eta}{2}(\hat{a}\rho_{ge} + \rho_{eg}\hat{a}^\dagger) - \Gamma_e \rho_{ee} \ . \tag{21}$$

$$\tag{22}$$

Note that in the weak excitation limit the excited state is almost empty every time. In particular we have:

$$|\rho_{ee}| \ll |\rho_{eg}| \ll |\rho_{gg}| \ . \tag{23}$$

The standard procedure for adiabatic elimination consist in neglecting the time derivative of ρ_{ee} and ρ_{eg}. This is means that this two terms adjust adiabatically to the slow variation of ρ_{gg}. The second approximation is to neglect the term ρ_{ee} in Eq.(20) so that is immediate to obtain:

$$\rho_{eg} = \frac{\Omega_0 \eta}{\Gamma_e} \hat{a} \rho_{gg} \ . \tag{24}$$

Plugging this result in Eq.(21) one gets:

$$\rho_{ee} = \frac{\Omega_0^2 \eta^2}{\Gamma_e^2} \hat{a} \rho_{gg} \hat{a}^\dagger \ . \tag{25}$$

This two result substituted into Eq.(19) give an expression for $\dot{\rho}_{gg}$:

$$\frac{d\rho_{gg}}{dt} = \Gamma \hat{a} \rho_{gg} \hat{a}^\dagger - \frac{\Gamma}{2} \left(\hat{a}^\dagger \hat{a} \rho_{gg} + \rho_{gg} \hat{a}^\dagger \hat{a} \right) \ , \tag{26}$$

where

$$\Gamma = \frac{\Omega_0^2 \eta^2}{\Gamma_e^2} \ , \tag{27}$$

is the effective damping rate of the motion. Note that Eq.(26) nearly corresponds to the motional density matrix($\rho_z = \rho_{gg} + \rho_{ee}$) because of the small lifetime of the excited state. As a result the effect of this mechanism is a cascade precess that brings the ion to its motional ground state($|g, 0\rangle$). Such a state is said to be the dark state for the system.

3.1 Additional remarks

One last important thing I want to point out is that the state $|g, 0\rangle$ is *decoherence-free*. In general a state $|\phi\rangle$ is said to be decoherence-free if it satisfy the following conditions[5]:

- $L|\phi\rangle = 0$, meaning that $|\phi\rangle$ is an eigenstate of the jump operator L with eigenvalue 0.
- $LH_a|\phi\rangle = 0$, where H_a is the Hamiltonian of the system.

When a general state falls in this eigenspace of L, it remains trapped in it forever and it will evolve under the effect of H_a remaining disentangled from the environment.

For sideband cooling purposes, it is necessary to look at the definition of the density matrix evolution Eq.(26) where the jump operator is $L \propto \hat{a}$. since that we are working in the interaction picture representation, the free evolution is frozen. Furthermore it is immediate to verify that $L|g, 0\rangle = 0$. From this it follows that the motional ground state is a decoherence-free state.

This final remark is of crucial importance because it gives the possibility of engineering several motional states just by properly choosing the right jump operator (see next chapters for more details).

3.2 A more general evolution

In the above derivation the recoil of the ion was not taken into account. This factor is of crucial importance because it can limit the efficiency of the process, leading to a system not perfectly cooled to its ground state.Therefore in every simulation I considered the general matrix evolution given by[4]:

$$\begin{aligned}\frac{d\rho}{dt} &= -i\,[H_l, \rho] + \\ &+ \Gamma_{eg}(2\sigma_-\rho\sigma_+ - \sigma_+\sigma_-\rho - \rho\sigma_+\sigma_-) + \\ &+ \Gamma_{eg}\frac{2}{5}\eta^2\sigma_+(2\hat{R}\rho\hat{R} - \hat{R}^2\rho - \rho\hat{R}^2)\sigma_- \ .\end{aligned} \tag{28}$$

The first line represent the usual density matrix evolution under the effect of the laser Hamiltonian H_l. The second row represent the spontaneous decay of the internal state (decay rate given by Γ_{eg}), while the third line contains information regarding the recoil of the ion.

It is important to notice that for simplicity the process is restricted to a one-dimensional atomic motion. Defined in this way $\hat{R}$ is the position operator for the ion, η is the LD parameter, while the factor $\frac{2}{5}$ comes from the normalization of the angular distribution of spontaneous emission $W(x)$(equal to $\frac{3}{4}(1+x^2)$ for dipole transition)[4]:

$$\alpha = \frac{2}{5} = \frac{1}{2}\int_{-1}^{1} dx\ x^2 W(x)\ . \tag{29}$$

The density matrix ρ is defined as a tensor product between the internal states and the motional states:

$$\rho = \rho_{internal} \otimes \rho_{motion}\ . \tag{30}$$

Of course it is computationally impossible to consider all the possible motional levels, therefore in all the simulations this term of the density matrix is truncated to a finite number (nHO). This value must be chosen carefully because the simulated motional state must be faithful representation of the real one.

3.3 Results

The simulation of the cooling process was done using a Matlab code. Important parameters to be defined are the decay rate $\Gamma_{e.g.}$ and the Rabi frequency Ω_r. Both of them are arbitrary

and depends on the strength of the field used; the first one depends on the coupling of the $|e\rangle \rightarrow |f\rangle$ transition (see Fig.2) and on the decay rate Γ_{fg} via Eq.16. Instead, the second one is defined as:

$$\Omega_r = \Omega_c \eta \ , \tag{31}$$

where Ω_c is the carrier transition.

An other relevant parameter is the one defining how many expansion terms of e^{ikx} are taken into account. For the LD approximation, where the whole theory holds, this parameter is set to 1. If interested in situation where the LD approximation is violated see the last chapter.

An example of output is shown in Fig.3. The starting point of the simulation is a doppler cooled calcium ion described by a thermal state with $\bar{n} = 2$.Due to the occupancy of lower the motional states, the LD approximation fits perfectly.

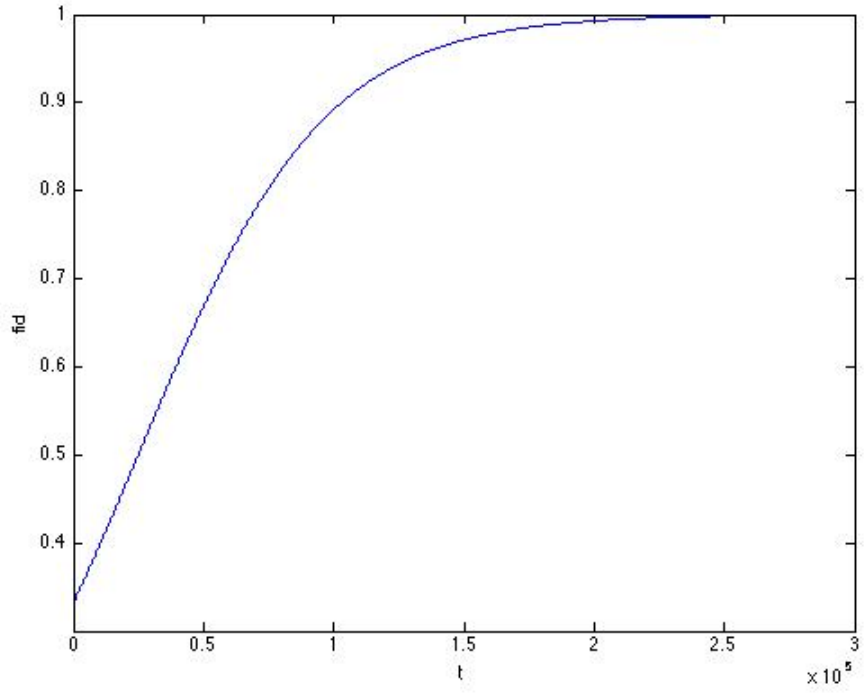

Figure 3: *Fidelity vs time* (time given in trap cycles). Starting point: thermal state with $\bar{n} = 2$.

In the case of interest Ω_r is chosen such that the $\frac{\pi}{2}$ carrier transition last $20\mu s$. There for it turns out that $\Omega_r = 0.011$ (measured in trap frequency unit). The decay rate is chosen

as $\Gamma = 0.01$ and no off-resonant terms are considered. The plot shows the $fidelity\ vs\ time$ (time given in trap cycles), where the fidelity is simply evaluated as:

$$fid(t) = Tr(\rho(t)\ \rho_{aim})\ , \tag{32}$$

where ρ_{aim} is the aimed state ($|g,0\rangle\langle g,0|$) and $\rho(t)$ is the initial system after a time t.

As visible from this example, it seems to be possible to reach the ground state of the motion with a very high fidelity. Note that the fidelity at $t = 0$ is ≈ 0.33 which is in agreement with the assumption of a thermal state with $\bar{n} = 2$. For a more rigorous approach it is probably necessary to take into account also off-resonant terms but, as will be shown in the next chapter, these doesn't influence the maximum fidelity in the case of interest (see Fig.6).

4 Coherent state preparation

Trapped ions are not only a powerful tool for quantum logic purposes; indeed, they can be also used to engineer several classical and non-classical states. In the this chapter I will show an interesting method to create a coherent state (a classical state) of the ionic motion starting from a purely quantum system. The process described also allow to create a decoherence free state (see Chapter 3.1).

In general a coherent state $|\alpha\rangle$ satisfies several properties. For our purposes I will only say that these states are eigenstates of the destroying operator $\hat{a}$ with eigenvalues α:

$$\hat{a}|\alpha\rangle = \alpha|\alpha\rangle\ , \tag{33}$$

and can be created applying a displacement operator $\hat{D}(\alpha)$ on the vacuum state $|0\rangle$

$$|\alpha\rangle = \hat{D}(\alpha)|0\rangle = e^{\alpha\hat{a}^\dagger - \alpha^*\hat{a}}|0\rangle\ . \tag{34}$$

An equivalent way of writing it, is using the representation in the basis of Fock states:

$$|\alpha\rangle = e^{\frac{|\alpha|^2}{2}} \sum \frac{\alpha^n}{\sqrt{n!}}|n\rangle\ , \tag{35}$$

which leads to a Poissonian probability distribution:

$$P(n) = e^{-|\alpha|^2}\frac{|\alpha|^{2n}}{n!} \tag{36}$$

with an average phonon number $\bar{n} = |\alpha|^2$ (see Fig.4) .

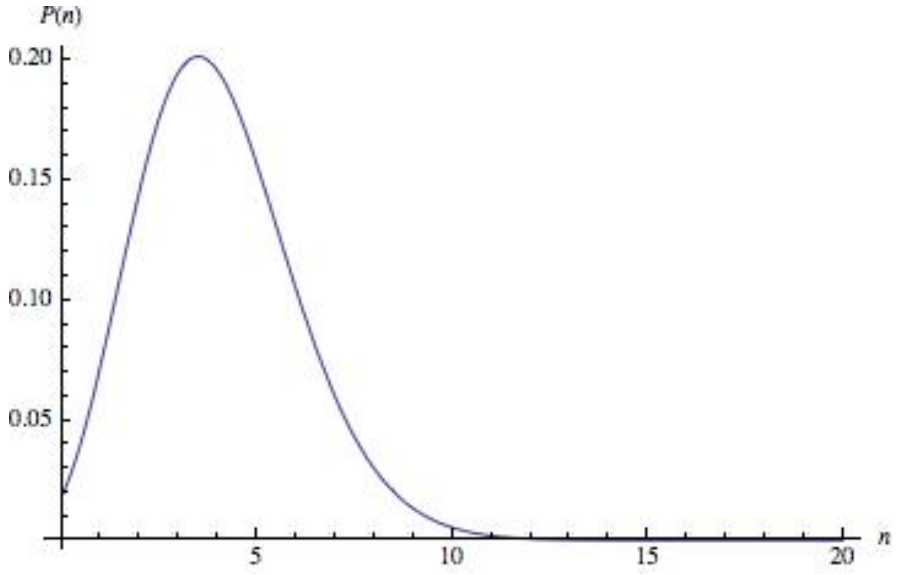

Figure 4: Plot of a coherent state with $|\alpha| = 2$.

Using the properties shown in Chap 3.1 and Eq.(33) it is possible to find a process that allows the creation and protection of a coherent state. First of all it is worth noting that $|\alpha\rangle$ satisfies the following:

$$(\hat{a} - \alpha\mathbb{1})|\alpha\rangle = 0 \ ; \tag{37}$$

this means that it is possible to protect a coherent state just by engineering a Lindblad operator L proportional to $\hat{a} - \alpha\mathbb{1}$. This is obtained by shining the system with two laser field: one at carrier frequency, with a Rabi frequency Ω_c and a second one at the first red sideband, with Rabi frequency $i\eta\Omega_r$. Therefore the Lindblad operator is[5]:

$$L = \frac{1}{\Gamma_e}\left(\Omega_c\mathbb{1} + i\eta\Omega_r\hat{a}\right) \ , \tag{38}$$

that by comparison with Eq.(33) gives a coherent amplitude defined by:

$$\alpha = \frac{i\Omega_c}{\Omega_r\eta} \ . \tag{39}$$

Given the previous definition it is easy to set up a simulation very similar to the one described in Chapter 3. In Fig.5 is shown a possible output. The Hamiltonian is described as the sum of two different Hamiltonian: the red sideband and the carrier. The simulation is implemented in a way such that one has to define the α parameter and the red sideband

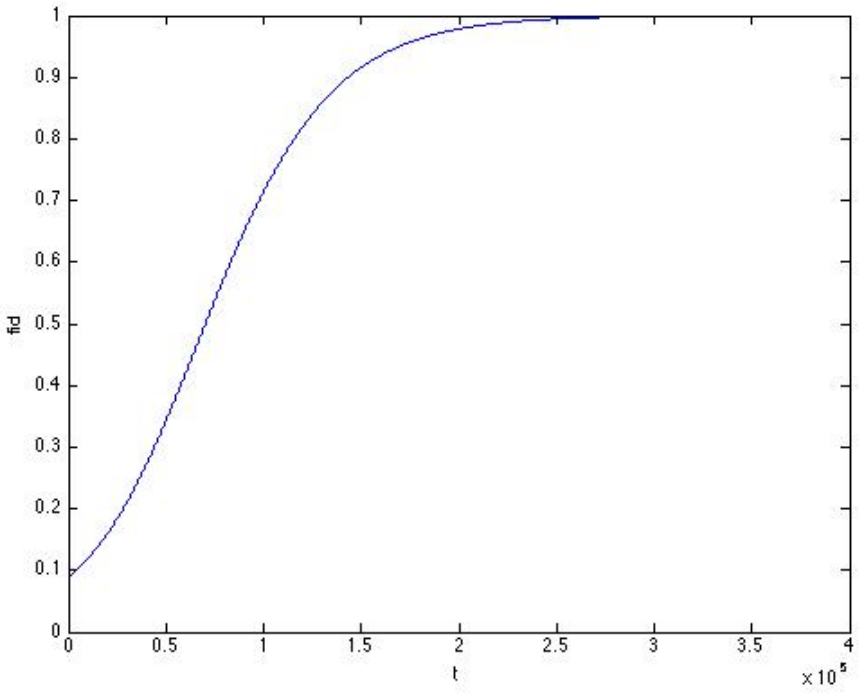

Figure 5: *Fidelity vs time* (time given in trap cycles). Starting point: thermal state with $\bar{n} = 2$. $\Omega_r = 0.011$, $\Gamma = 0.01$ and $\alpha = 2$.

Rabi frequency Ω_r. Therefore the Ω_c term is derived from Eq.(39) as:

$$\Omega_c = \frac{1}{i}\Omega_r \eta \alpha \ . \tag{40}$$

The reason why one defines Ω_r instead of Ω_c is that for small values of α ($\alpha < 1/\eta \approx 14$ for calcium ion) $\Omega_r > \Omega_c$.
On one hand side, having high values of Ω_r is an advantage because it reduces the time needed to gets to the final state, but on the other hand side it complicates the process because one has to consider also the AC Stark shift and the off resonant terms. In all the simulation the AC Stark shift is always included, also when it is negligible, while I typically consider only only resonant terms to reduce the computational time.

To have an idea of the influences of the off-resonant terms on the maximum fidelity it is possible to do a simulation where the first off-resonant term is considered and all the other parameters are fixed except for Ω_r which, instead, is increased at every step of the

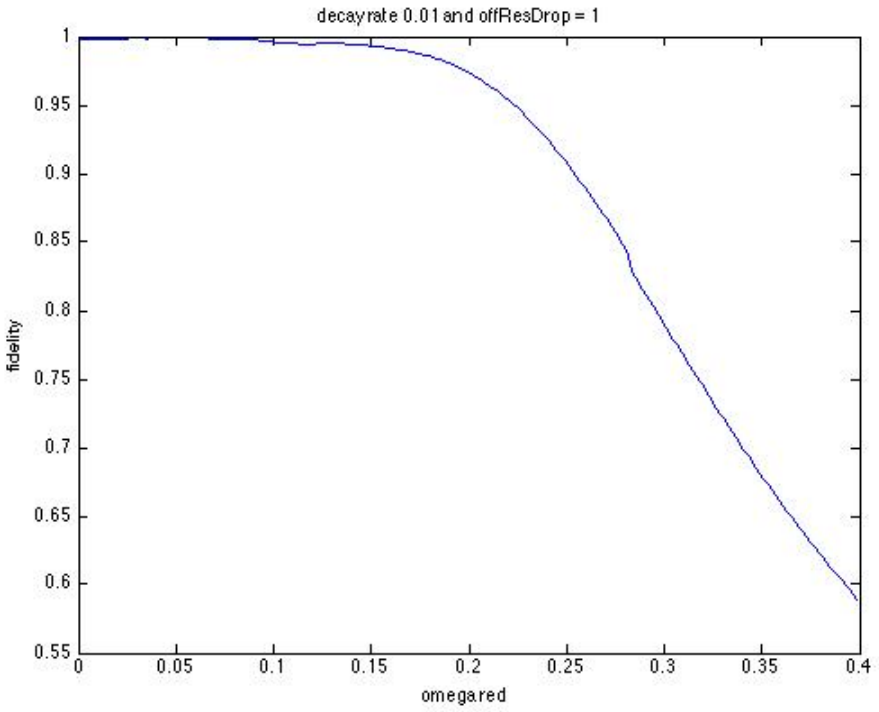

Figure 6: *Fidelity vs* Ω_r. Starting point: thermal state with $\bar{n} = 2$. Parameters: $\alpha = 1$, $\Gamma = 0.01$. 1 off-resonant term considered

simulation. The maximum reached fidelity is stored and plotted in a graph similar to Fig.6.

The plot shows a drop of the maximum fidelity when Ω_r is approximately 20 times bigger then Γ. This drop was expected because in the theory explained in Chapter 2 and 3, especially when talking about the adiabatic elimination, we made the assumption that $\Omega \ll \Gamma$.

Another issue one has to consider is, as always, the LD approximation: from Eq.(36) one can immediately see that coherent states with a large amplitude are spread onto highly excited states. This means that it is not possible to create such states without breaking the LD approximation. For a more detailed explanation see the last chapter of this report.

As a final remark I can say that thanks to these two last remarks the simulation output shown in Fig.5 is in perfect agreement with the above approximation. Therefore I expect that it will be possible to realize it experimentally with a very high fidelity.

5 Squeezed state preparation

In the previous Chapter it was shown a method to engineer and protect a classical state of motion. In the last few decades people have been growing interest in preparing also non-classical state of quantum system in order to study fundamental properties of quantum mechanics. An example of these are Schrodinger cat states that are a "macroscopical" superposition of two opposite classical states: $|\Psi\rangle = C(|\alpha\rangle + |-\alpha\rangle)$. Such states can be engineered using an approach similar to the one used in the previous chapters, but for the purpose of this report they are not relevant.

In this chapter I will show other types of non classical states called *squeezed states*. The most important feature of such states is that the electric field variance lies between:

$$0 \leq (\Delta E)^2 \leq \frac{1}{4} \ . \tag{41}$$

Thanks to this property it is possible to distinguish squeezed states from coherent states, whose electric field invariance is always equal to $\frac{1}{4}$.

In this report I will show a simulation to create a particular squeezed state called *squeezed vacuum*. Such a state is defined by applying the squeezing operator ($\hat{S}$) onto the vacuum:

$$|\zeta\rangle = \hat{S}(\zeta)|0\rangle = e^{\frac{1}{2}\zeta^* \hat{a}^2 - \frac{1}{2}\zeta (a^\dagger)^2} \ , \tag{42}$$

where ζ is the complex squeeze parameter defined by $\zeta = se^{i\theta}$.
A very useful property of the squeezing operator is that:

$$\hat{S}^\dagger(\zeta)\hat{a}\hat{S}(\zeta) = \hat{a}\cosh(s) - \hat{a}^\dagger e^{i\theta}\sinh(s) \ . \tag{43}$$

Given these features it is possible to find a way to create such states using laser fields. There exists two ways to derive it: the first one is to note that

$$(\hat{a}\cosh s - \hat{a}^\dagger e^{i\theta}\sinh s)|\zeta\rangle = 0 \ , \tag{44}$$

which means that we shall use a blu sideband laser field (jump operator $L_1 \propto \hat{a}^\dagger$) and a red sideband laser (jump operator $L_2 \propto \hat{a}$). This method is the one used in the previous chapter, so it is probably more interesting to look at another way of obtaining this conclusion.

When creating the squeezed vacuum with some kind of laser field the Hamiltonian we obtain should be something like

$$H \propto \sigma_+ \hat{S}^\dagger(\zeta)\hat{a}\hat{S}(\zeta) + h.c. \ . \tag{45}$$

Using Eq.(43) the previous statement becomes:

$$H \propto \sigma_+(C_1\hat{a} + C_2\hat{a}^\dagger) + h.c. \ , \tag{46}$$

where C_1 and C_2 satisfy:

$$\frac{|C_1|}{|C_2|} = \frac{1}{\tanh s} \tag{47}$$

$$\arg\left(\frac{C_1}{C_2}\right) = \theta \ . \tag{48}$$

The first thing to note is that we obtained a field Hamiltonian that is the sum of a red sideband term and a blu one. Secondly, the two last equation give a strict relationship between the two Rabi frequency where $C_1 = \Omega_r$ and $C_2 = \Omega_b$.

5.1 Additional remarks.

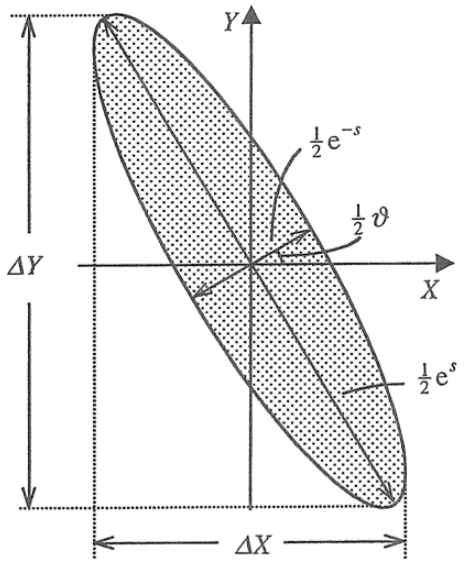

Figure 7: Squeezed vacuum state representation.[3]

Before going on to describe the result of the simulation, I just want to point out few additional remarks. First of all it is worth noting that although we consider the squeezed vacuum state, the average phonon number isn't null but it can be shown that[3]:

$$\bar{n} = \sinh^2 s \ , \tag{49}$$

and from this it follows that the variance is:

$$(\Delta n)^2 = 2\bar{n}(\bar{n}+1)\ . \tag{50}$$

As always this is of crucial importance because the entire theory is based on the LD approximation; therefore we want this value to be small enough (for a better explanation see next Chapter).

In general a squeezed state can be represented in a graph where the two axis (X,Y) are the quadrature components. It is easy to show that the mean value of the these two is always equal to 0 but the variance is instead[3]:

$$(\Delta X)^2 = \frac{1}{4}(e^{2s}\sin^2\frac{\theta}{2} + e^{-2s}\cos^2\frac{\theta}{2}) \tag{51}$$

$$(\Delta Y)^2 = \frac{1}{4}(e^{2s}\cos^2\frac{\theta}{2} + e^{-2s}\sin^2\frac{\theta}{2})\ . \tag{52}$$

Therefore the squeezed state in such plane is represented as an ellipse like Fig.7. The same plot can also be done for the vacuum field, but in this case we will obtain a circle centered in the origin and with a radius of $\frac{1}{4}$.

This means that it is possible to understand the strength of the squeezing just by looking at the axis ratio of the ellipse. This value is equal to e^{2s}.

5.2 Simulation and results.

We now have all the necessary ingredients to perform the simulation. As before, to better control the system I choose the squeezed state I want to achieve (defining s and θ) and the value of Ω_r.

Fig.8 shows that a possible outcome of the simulation. As always, it shows that it is possible to reach the desired state. Further analysis on these states will be provided in the next section where I talk about the LD approximation. As we will see the it turns out that the squeezed state is more robust than the coherent one.

6 The Lamb-Dicke approximation

As already mentioned in Chapter 2, the Lamb-Dicke approximation consists in neglecting all the terms in the expansion of $e^{ik\cdot R}$ except for the lowest one. Many qubit gates rely on this assumption, so it is of crucial importance being able to work in this regime in order to have the maximum gate fidelity.

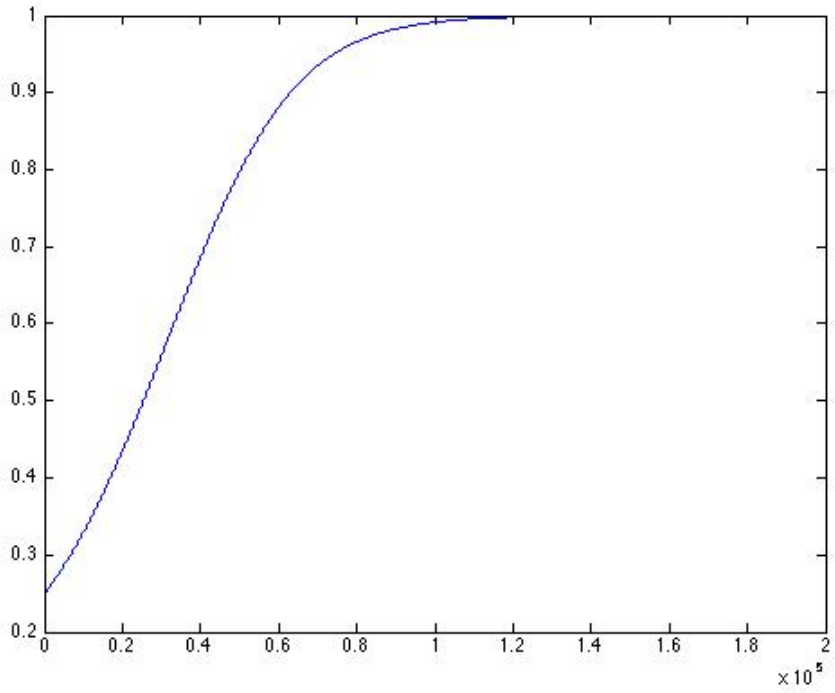

Figure 8: *Fidelity vs time* (time given in trap cycles). Starting point: thermal state with $\bar{n} = 2$. $\Omega_r = 0.011$, $\Gamma = 0.001$ and $s = 1$, $\theta = \frac{\pi}{2}$. Axis ratio= 7.39.

This approximation is indeed one of the most source of errors for many qubit gates[2]; these, indeed work with a very high fidelity only in this regime. To understand the origin of the problem consider the expansion of $e^{ik\cdot R}$ when applying a red sideband field:

$$ik \cdot R \approx i\eta(\hat{a} + \hat{a}^\dagger)(1 + \frac{\eta^2}{2!}(2\hat{n} + 1) + \dots) \ . \tag{53}$$

This shows that the Rabi frequency is strongly dependent on the phonon number state. As a result one has to pay attention when assuming the LD approximation while working with states with a large motional variance. This is the case of coherent and squeezed states with large α and s.

6.1 Coherent Vs. Squeezed states

We now have the tools to calculate the limit of the theory explained in the previous chapters. Consider as a first example the coherent state preparation of Chapter 4. Depending on α

the variance of the state is

$$(\Delta n)^2 = |\alpha|^2 \ . \tag{54}$$

This means that when increasing α the probability distribution spreads on a large number of motional states each of them with a different Rabi frequency. As a result we expect to have a preparation fidelity that decreases as α increase. In order to test this idea it is

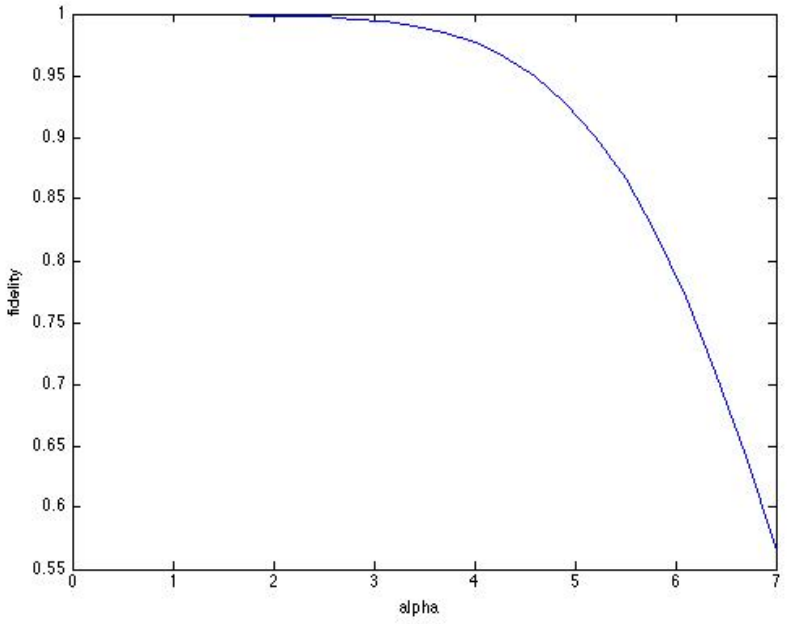

Figure 9: *Fidelity vs* α . Starting point: thermal state with $\bar{n} = 2$. $\Omega_r = 0.05$, $\Gamma = 0.01$. Expansion of e^{ikR} to the third order.

possible to make a simulation where we calculate the maximum value of fidelity for different coherent amplitude α. Fig.9 shows the output of this simulation, in which all parameter are fixed except for α that varies from 0 to 7. In this case the e^{ikR} term is expanded till the third order.
From the plot it is immediate to see that there is a drop in fidelity around $\alpha = 4$ that means a variance of:$(\Delta n)^2 = 16$. From this simulation we can conclude that it is possible to create only coherent states with a small amplitude.

The same process can be applied to squeezed state preparation. The output is shown in Fig.10. in this case what varies is the squeezing amplitude r that goes from 0 to 1.7. Remembering Eq.(49) and Eq.(50) it is immediate to observe that the mean photon number goes from $\bar{n} = 0$ to $\bar{n} \approx 7$ and the variance form $(\Delta n)^2 = 0$ to $(\Delta n)^2 \approx 112$.

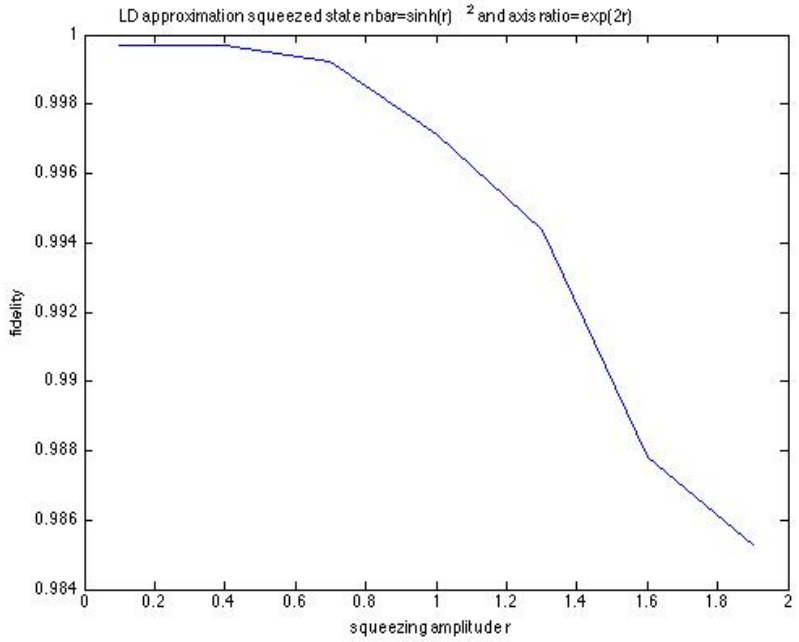

Figure 10: *Fidelity vs* r (squeezing amplitude). Starting point: thermal state with $\bar{n} = 2$. $\Omega_r = 0.05$, $\Gamma = 0.01$. Expansion of e^{ikR} to the third order.

As visible form Fig.10 the maximum fidelity remains very high for every value for r reflecting that this state is very robust although the LD approximation is violated.

Therefore, from these simulations, it seems that coherent states are much more robust than coherent ones. The reason for this must be searched in the definition of α (Eq.(39)) and r(Eq.(47)). In particular we can observe that

$$\alpha \propto \frac{\Omega_c}{\Omega_r} \ , \tag{55}$$

while

$$r \propto \text{arctanh}(\frac{\Omega_b}{\Omega_r}) \ . \tag{56}$$

In the Lamb-Dicke regime $\Omega_r^{(LD)}(n) \propto -i\eta\sqrt{n}$, $\Omega_b^{(LD)}(n) \propto -i\eta\sqrt{n+1}$ and $\Omega_c(n)^{(LD)} \propto 1$, where n is the phonon number state. A first way of checking whether squeezed states are more robust is to see how α and r change when considering higher term in the expansion. As an example consider the case where you expand the exponential till the fifth order, then

it follows that:

$$\Omega_c^{(5)} \propto 1 - \frac{\eta^2}{2}(2n+1) + \frac{\eta^4}{8}(2n^2+2n+1) \tag{57}$$

$$\Omega_r^{(5)} \propto i\eta\sqrt{n}[-1 + \eta^2\frac{n}{2} - \frac{\eta^4}{5!}(10n^2-4n+1)] \tag{58}$$

$$\Omega_b^{(5)} \propto i\eta\sqrt{n+1}[-1 + \eta^2\frac{n+1}{2} - \frac{\eta^4}{4!}(2n^2-4n+3)] \ . \tag{59}$$

From this we can plot the ratio $r^{(LD)}/r^{(5)}$ and $\alpha^{(LD)}/\alpha^{(5)}$ (see Fig.11). From the plot it is

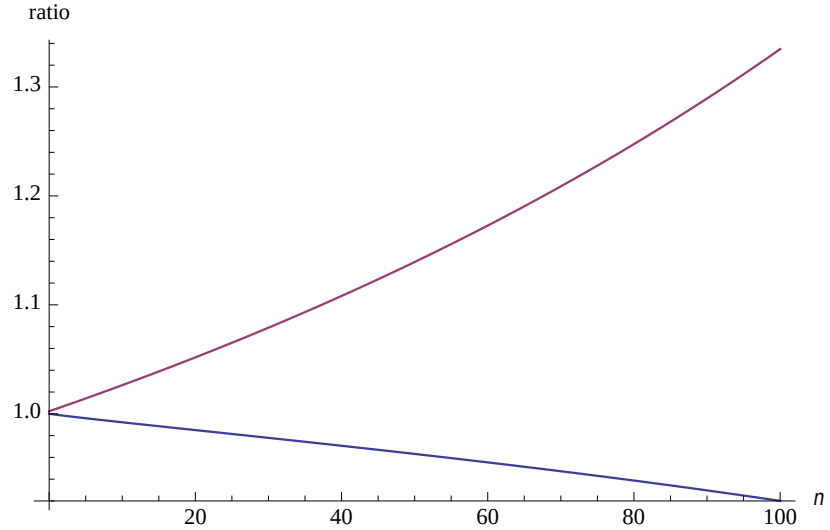

Figure 11: Blu line: $r^{(LD)}/r^{(5)}$ ratio, Red line:$\alpha^{(LD)}/\alpha^{(5)}$

visible that for $0 \leq n \leq 100$ the ratio for the squeezed state remain nearer to 1 than the ratio for the coherent state.

The previous approach was just approximated. There exist another method that is exact and can predict the ratio for every value of n. Indeed, it is possible to show that [6]

$$e^{i\eta(\hat{a}e^{i\omega_z t}+\hat{a}^\dagger e^{-i\omega_z t})} = |n'\rangle\langle n|e^{-\frac{\eta^2}{2}}\left(\frac{n_<!}{n_>!}\right)^{\frac{1}{2}}\eta^{|n'-n|}L_{n_<}^{|n'-n|}(\eta^2)e^{i\omega_z(n'-n)t} \ , \tag{60}$$

where $n_>$ is the greatest between n' and n. This means that in the case of the carrier transition ($n' = n$):

$$e^{\cdots} = |n\rangle\langle n|e^{-\frac{\eta^2}{2}}L_n^0(\eta^2) \ , \tag{61}$$

for the red sideband transition ($n' = n-1$)

$$e^{\cdots} = |n-1\rangle\langle n|e^{-\frac{\eta^2}{2}}\left(\frac{1}{n}\right)^{\frac{1}{2}}L_{n-1}^1(\eta^2)e^{i\omega_z t}\eta \ , \tag{62}$$

while for the blu sideband transition ($n' = n + 1$):

$$e^{\cdots} = |n+1\rangle\langle n| e^{-\frac{\eta^2}{2}} \left(\frac{1}{n+1}\right)^{\frac{1}{2}} L_n^1(\eta^2) e^{-i\omega_z t}\eta \ . \tag{63}$$

Repeating the same process done before using these last equation one obtain the plot shown in Fig.12. Looking at the graph it is possible to observe two things: first of all that there are diverging point which corresponds to zeros in the Laguerre polynomials. Secondly, except for the point where the ratio diverges, the squeezed state is much more robust than the coherent one.

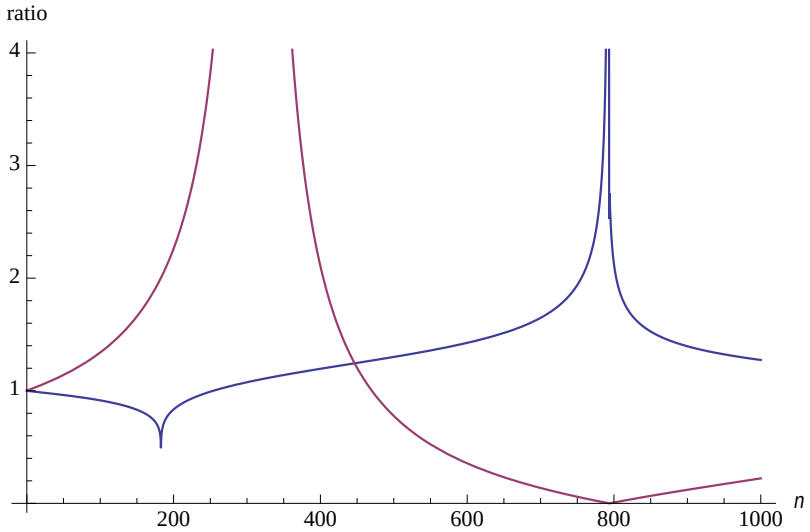

Figure 12: Blu line: $r^{(LD)}/r^{(exact)}$ ratio, Red line:$\alpha^{(LD)}/\alpha^{(exact)}$

Computationally speaking it can be difficult to evaluate the exact expression of the exponential term for every value of n. This is due to computational problems in evaluating the factorial terms contained in the expresso of the Laguerre polynomials. Therefore for $n \to \infty$ we can use the following approximation[6]:

$$e^{-\frac{x}{2}} x^{\frac{a}{2}} L_n^a(x) = \frac{\Gamma(n+a+1)}{(\nu/4)^{\frac{a}{2}} n!} J_a((\nu x)^{\frac{1}{2}}) \ , \tag{64}$$

where J_a is the Bessel function, $\nu = 4n + 2a + 2$ and $\Gamma(\dots)$ is the Euler gamma function. This approximation can be applied to our purposes noting that in the case of a carrier transition

$$e^{\cdots} = J_0((4n+2)^{\frac{1}{2}}\eta) \ , \tag{65}$$

for the red sideband transition we obtain

$$e^{\cdots} = J_1(2(n)^{\frac{1}{2}}\eta)e^{i\omega_z t} \ , \tag{66}$$

and for the blu sideband transition

$$e^{\cdots} = J_1((4n+4)^{\frac{1}{2}}\eta)e^{-i\omega_z t} \ . \tag{67}$$

7 Conclusion

In this report I have shown different methods to engineer the motional states of the ion working in the dispersive regime. Simulations show that it is possible to create these states with a very high fidelity as long as the LD approximation is valid. Furthermore I've demonstrated both theoretically and computationally that squeezed motional states are much more robust than coherent one. This has to do with the definition of the squeezing amplitude that is proportional to the ratio of the blu and the red sideband Rabi frequency. This is different from the coherent one because this is proportional to the ratio between the carrier the red sideband frequency.

References

[1] Wineland et al, *Experimental Issues in Coherent Quantum-State Manipulation of Trapped Atomic Ions*, Journal of Research of of the National Institute of Standards and Technology, Volume 103, Number 3 (1998)

[2] Lecture Notes of *Cavity QED and ion trapping* course held by Jonathan Home.

[3] Loudon *The Quantum theory of Light* third edition, Oxford Pubblication.

[4] Cirac et al. *Laser cooling of trapped ions in a standing wave*, Phys. Rev. A Volume 46, Number 5 (1992)

[5] Haroche, Raimond *Exploring the quantum*, Oxford Graduate Text.

[6] Wineland, Itano *Laser cooling of atoms*, Phys Rev A. Volume 20(1979).